TẠP CHÍ KHOA HỌC
TRƯỜNG ĐẠI HỌC QUY NHƠN

Nghiên cứu đặc trưng cấu trúc và hoạt tính quang xúc tác phân hủy dung dịch RhB của vật liệu màng C/g-C_3N_4/PVDF

Nguyễn Thị Lan[1,*], Trịnh Ngọc Đạt[2], Lê Vũ Trường Sơn[2], Đinh Thanh Khẩn[2], Huỳnh Văn Nam[1], Đinh Quốc Việt[1], Nguyễn Minh Vương[1], Nguyễn Tấn Lâm[3,*], Nguyễn Văn Thắng[1], Phan Thị Thùy Trang[1]

[1]Khoa Khoa học Tự nhiên, Trường Đại học Quy Nhơn, Việt Nam
[2]Trường Đại học Sư phạm, Đại học Đà Nẵng, Việt Nam
[3]Phòng Thanh tra, Trường Đại học Quy Nhơn, Việt Nam

Ngày nhận bài: 11/01/2025; Ngày sửa bài: 30/05/2025;
Ngày nhận đăng: 06/06/2025; Ngày xuất bản: 28/06/2025

TÓM TẮT

Vật liệu composite carbon/graphit carbon nitride/polyvinylidene fluoride (C/g-C_3N_4/PVDF) có cấu trúc dị thể được tổng hợp thành công bằng phương pháp đảo pha đơn giản. Hình thái, cấu trúc và hoạt tính quang xúc tác của các hạt C/g-C_3N_4 và màng composite đã được đánh giá. Nhờ hiệu ứng hiệp trợ giữa carbon và g-C_3N_4 được phân tán trên màng PVDF đóng vai trò là chất xúc tác đã cải thiện một cách đáng kể khả năng phân hủy chất màu rhodamine B trong dung dịch. Cụ thể, vật liệu C/g-C_3N_4/PVDF thể hiện hiệu suất quang xúc tác cao nhất (H = 89%) so với các vật liệu g-C_3N_4/PVDF (H = 45,92%) sau 160 phút chiếu sáng dưới vùng ánh sáng khả kiến. Với phương pháp đưa vật liệu lên màng đã khắc phục được những nhược điểm vốn có của các loại xúc tác truyền thống như khó thu hồi và khả năng tái sử dụng xúc tác với hiệu suất thấp sau nhiều chu kì. Vì vậy, nghiên cứu này dự kiến sẽ được mở rộng một cách triển vọng trong lĩnh vực xúc tác quang.

Từ khóa: C*omposite, polyvinylidene fluoride, C/g-C_3N_4/PVDF, rhodamine B, chất xúc tác quang.*

**Tác giả liên hệ chính.*
Email: nguyentanlam@qnu.edu.vn, nguyenthilan@qnu.edu.vn

QUY NHON UNIVERSITY
JOURNAL OF SCIENCE

Study on structure characteristics and the photocatalytic activities degradation of RhB solution on C/g-C_3N_4/PVDF membrane material

Nguyen Thi Lan[1,*], Trinh Ngoc Dat[2], Le Vu Truong Son[2], Dinh Thanh Khan[2], Huynh Van Nam[1], Dinh Quoc Viet[1], Nguyen Minh Vuong[1], Nguyen Tan Lam[3,*], Nguyen Van Thang[1], Phan Thi Thuy Trang[1]

[1]Faculty of Natural Sciences, Quy Nhon University, Vietnam
[2] The University of Da Nang, University of Science and Education, Viet Nam
[3]Inspection office, Quy Nhon University, Vietnam

Received: 11/01/2025; Revised: 30/05/2025;
Accepted: 06/06/2025; Published: 28/06/2025

ABSTRACT

Heterogeneous carbon/graphite carbon nitride/polyvinylidene fluoride (C/g-C_3N_4/PVDF) composite materials were successfully synthesized by a simple phase inversion method. The morphology, structure, and photocatalytic activity of C/g-C_3N_4 particles and composite films were evaluated. Thanks to the synergistic effect between carbon and g-C_3N_4 dispersed on the PVDF membrane acting as a catalyst, the ability to decompose rhodamine B dye in solution was significantly improved. Specifically, the C/g-C_3N_4/PVDF material exhibited the highest photocatalytic efficiency (H = 89%) compared to the g-C_3N_4/PVDF material (H = 45,92%) after 160 minutes of illumination under visible light. The method of putting materials on the membrane has overcome the inherent disadvantages of traditional catalysts, such as difficulty in recovery and the ability to reuse the catalyst with low efficiency after many cycles. Therefore, this study is expected to be prospectively extended in photocatalysis for the treatment of polluted water.

Keywords: C*omposite, polyvinylidene fluoride, C/g-C_3N_4/PVDF, rhodamine B, photocatalyst.*

1. INTRODUCTION

Photocatalysis has emerged as one of the most promising green technologies thanks to its environmental benefits, cost-effectiveness, and high efficiency. It has found widespread applications in environmental management and energy conversion.[1,2] A crucial aspect of advancing photocatalytic technology lies in developing new photocatalysts that efficiently harness solar energy, addressing the pressing need for environmental remediation today.

Rhodamine B (RhB) is one of the most popular dyes for the printing, textile, and leather industries, which could cause environmental pollution if not treated appropriately. Various technologies have been explored recently to develop effective methods for completely removing pharmaceutical and dye compounds from water.[3,4] Among these, advanced oxidation processes (AOPs) have been identified as a promising solution for treating difficult-to-degrade compounds. AOPs, remarkably

**Corresponding author.*
Email: nguyentanlam@qnu.edu.vn, nguyenthilan@qnu.edu.vn

https://doi.org/10.52111/qnjs.2025.19310

heterogeneous photocatalysis, have received significant due to their high efficiency in removing pharmaceuticals.[5,6] Photocatalysts absorb photons from an external light source to generate electron-hole pairs, participating in redox reactions. Among the various photocatalysts, graphitic carbon nitride (g-C_3N_4) has emerged as a promising metal-free, layered material easily synthesized by thermal condensation using inexpensive and abundant organic precursors in soil, such as urea.[7]

As a narrow band gap semiconductor (2.7 eV), g-C_3N_4 demonstrates stable physicochemical properties, excellent thermal stability, and remarkable photoelectron transfer capabilities. Additionally, it is non-toxic, easy to store, and can be obtained from various sources.[8] Recently, g-C_3N_4 has become an optimal choice for forming heterostructured materials with wide-band gap semiconductors. For example, Wang et al. developed a unique in situ microwave-assisted synthesis method to fabricate N-TiO_2/g-C_3N_4 composites, which showed significant improvements in photocatalytic activity.[9] Similarly, Miranda et al. successfully obtained g-C_3N_4/TiO_2 composites with high photoactivity by combining hydrothermal and sintering methods, achieving a final phenol conversion rate of approximately 90%.[10] However, g-C_3N_4 has shortcomings, such as a small specific surface area and a high recombination rate of photogenerated electron-hole pairs. To overcome this drawback, many methods have been applied to modify g-C_3N_4, such as preparing g-C_3N_4 in capillary structures and modifying g-C_3N_4 by doping techniques or grafting with other semiconductors to composite materials. [11,12]

Polyvinylidene fluoride (PVDF) is widely used for membrane fabrication due to its high mechanical strength, chemical resistance, and thermal stability.[13,14] Several g-C_3N_4-PVDF membranes have been developed and successfully applied in studies aimed at removing pollutants from water in continuous flow mode, with photocatalysts serving as self-cleaning materials that exhibit antifouling properties.[15,16]

The main objective of this study is to modify the surface of PVDF membranes with g-C_3N_4. The performance of the modified membranes was evaluated in the degradation of Rhodamine B dye.

2. EXPERIMENTAL

2.1. Material synthesis

Chemicals: All chemicals used for material synthesis include potassium hydroxide (KOH, 90%), hydrochloric acid (HCl, 37%), polyvinylidene fluoride (PVDF), N-Methy-2-pyrrolidone (NMP) urea ($CO(NH_2)_2$, ≥99%) (Sigma-Aldrich) and rhodamine B ($C_{28}H_{31}ClN_2O_3$) Merck

2.2. Materials synthesis

2.2.1. Synthesis of g-C_3N_4

Ten grams of the precursor urea was finely ground and transferred into a ceramic cup. The cup was then heated in a furnace at 550 °C with a heating rate of 10 °C/min under an Ar atmosphere for one hour. The obtained powder was washed with water, dried, and ground. The sample denoted g-C_3N_4.

2.2.2. Synthesis of C/g-C_3N_4 membrane material

A mixture of urea (15 g) and C[17] (0.1 g) was dispersed in a water-alcohol solution (1:1 ratio) and then subjected to ultrasonic vibration for 30 minutes. The mixture was continuously stirred at 60 °C until the water and alcohol wholly evaporated. The resulting solid was ground and heated in Argon gas at 550 °C for 1 hour. The product was washed, filtered, and dried at 80 °C for 12 hours to obtain the final product, C/g-C_3N_4.

2.2.3. Synthesis of C/g-C_3N_4/PVDF membrane material

Add 0.1 grams of C/g-C_3N_4 material to a glass jar with a lid, then add 5 mL of N-Methyl-2-pyrrolidone (NMP). Sonicate the mixture for 10 minutes, followed by stirring for 30 minutes. Afterward, continue sonicating for another 20 minutes and stir for 20 minutes. Next, add 0.646 grams of polyvinylidene fluoride (PVDF) and

stir the mixture at 40 °C for 4 hours. Allow the mixture to stand for 3 hours. Use a stainless steel knife (250 µm x 15 cm) to evenly roll the mixture onto a glass surface to form a composite film. Quickly immerse the glass with the film into the water to perform the phase inversion process.[17] The resulting product is denoted as C/g-C_3N_4/PVDF.

The process for dispersing g-C_3N_4 onto PVDF polymer is carried out similarly, and the product obtained is denoted as g-C_3N_4/PVDF.

2.3. Material characterization

The synthesized materials were characterized using several techniques. Infrared spectroscopy IR was performed on a Shimadzu IR Prestige-21). The crystal phase was analyzed by X-ray diffraction (XRD) using a Siemens D-500 Bruker system. Scanning electron microscopy (SEM) and X-ray energy dispersive spectroscopy (EDS) were conducted using a JSM-7600F device. Photoluminescence (PL) spectra were measured on a Hitachi F-7000 instrument with an excitation wavelength of 360 nm.

2.4. Photocatalytic evaluation

The photocatalytic activity of the obtained materials was evaluated by the decomposition of Rhodamine B (RhB) in an aqueous solution under visible light irradiation. Materials membrane containing 0.1 g of the photocatalyst was added to 100 mL of RhB solution with a concentration of 10 mg/L and stirred in the dark for 30 minutes to achieve adsorption-desorption equilibrium. The photocatalytic process was then initiated under a 30W LED light. Every 20 minutes, 5 mL of the solution was centrifuged to remove the solid part. The concentration of RhB in the solution was determined on a UV-Vis meter (CE-2011) at a wavelength of 553 nm.

3. RESULTS AND DISCUSSION

3.1. Material characteristics

XRD patterns were used to determine the crystalline phase of g-C_3N_4/PVDF and C/g-C_3N_4/PVDF composites, as shown in Figure 1a.

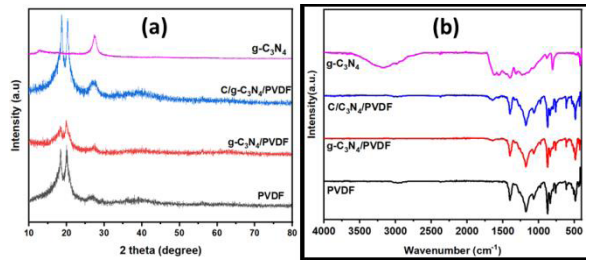

Figure 1. (a) XRD and (b) FT-IR patterns of PVDF, g-C_3N_4, g-C_3N_4/PVDF, and C/g-C_3N_4/PVDF.

PVDF is a semi-crystalline polymer with two main crystalline phases, α and β.[18,19] The results in Figure 1 indicate three characteristic peaks at 18.5°, 20.1°, and 26.7°, which are assigned to the reflection planes of (020), (110), and (021), corresponding to the α crystalline phase. When g-C_3N_4 or C/g-C_3N_4 were added to the PVDF polymer to form g-C_3N_4/PVDF and C/g-C_3N_4/PVDF composites, no significant change was observed compared to the pure PVDF sample. The three peaks attributed to the reflections of PVDF remain at nearly the same position but with varying intensities. The XRD pattern of g-C_3N_4 (Figure 1a) shows two characteristic peaks at 27.6° and 13.1° corresponding to the (002) and (100) reflection planes of graphite-structured materials.[20] In addition, the characteristic peak at 27.6° corresponding to the (002) plane of g-C_3N_4 appears in both the g-C_3N_4/PVDF and C/g-C_3N_4/PVDF samples (Figure 1a). The peak at 27.6° corresponding to the (002) plane of g-C_3N_4 is believed to result from the alternating stacking of conjugated aromatic units, similar to graphite structure.[21] The peak at 13.1° of g-C_3N_4 was not seen in the XRD patterns of g-C_3N_4/PVDF and C/g-C_3N_4/PVDF materials, possibly due to the small amount of g-C_3N_4 in the sample. The diffraction peaks of the C/g-C_3N_4/PVDF composite are more intense than those of the g-C_3N_4 sample, likely due to carbon increasing the intensity of the peaks in this material sample.

FT-IR spectra were employed to characterize the chemical bond characteristics of the samples, and the results are presented in Figure 1b. The FTIR spectrum of g-C_3N_4

https://doi.org/10.52111/qnjs.2025.19310

shows broad shoulder absorption bands at 3187 cm^{-1} corresponding to the stretching vibrational pattern of N-H in the incompletely condensed amine group or OH of the adsorbed water. In addition, there are some dominant, strong bands in the 1100–1700 cm^{-1} region in the IR spectrum, corresponding to the characteristic vibrational pattern of CN heteroaromatic rings. Specifically, the peaks around 1639 cm^{-1} and 1574 cm^{-1} can be attributed to the characteristic vibrational pattern of C=N bonds, while the peaks at 1247 cm^{-1} to 1458 cm^{-1} are assigned to the stretching vibrational pattern of C-N bonds in conjugated aromatic rings. The bands at 1325 cm^{-1} and 1247 cm^{-1} correspond to the valence vibrations of the C-N(-C)-C bridging units with a fully condensed system or C-NH-C with a partially condensed system. In addition, a sharp absorption band at 820 cm^{-1} is attributed to the deformation vibrations of the N-H groups of the triazine units. [22,23].

The FTIR spectrum of the PVDF membrane shows that the peak at 763 cm^{-1} corresponds to the bending vibration of the CF_2 group. The peaks at 794 and 977 cm^{-1} are attributed to the shaking vibration of the CF_2 group, while the peak at 1170 cm^{-1} is associated with the valence vibration of the CF_2 group.[24,25] The peak at 1413 cm^{-1} is deemed to be the valence vibration of the C-H functional group. In addition, the PVDF sample exhibits peaks at 875, 615, 531, and 490 cm^{-1}, all of which correspond to PVDF's α phase crystal structure.[26] For the composite membrane materials g-C_3N_4/PVDF and C/g-C_3N_4/PVDF, the peak appearing at 1639 cm^{-1} is attributed to the valence vibration of the C=N group.[27] The peaks at 2979 and 1411 cm^{-1} are assigned to the valence and deformation vibrations of the CH_2 group, respectively. In addition, the peak at 1181 cm-1 vibration is related to the valence vibration of the CF_2 group.[28]

The SEM images reveal that the surface of pure PVDF (Figure 2a) exhibits a homogeneous morphology. In comparison, the SEM image of g-C_3N_4/PVDF (Figure 2b) shows numerous voids between g-C_3N_4 and polymer chains, which are formed due to the particle distribution during the sample preparation. The SEM image of the C/g-C_3N_4/PVDF composite (Figure 2c) shows that many small particles are evenly dispersed on the PVDF substrate. These observations confirm that the presence of carbon in the composite sample influences the voids between particles and polymer chains.[21]

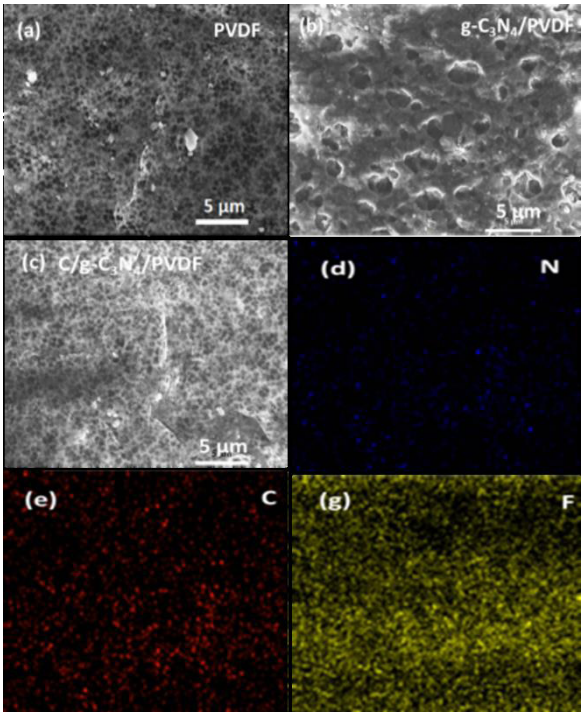

Figure 2. FE-SEM images of (a) PVDF, (b) g-C_3N_4/PVDF, (c) C/g-C_3N_4/PVDF, (d) mapping images of N, (e) C and (g) F elements.

The EDX spectrum in Figure 3 was used to identify the elements in the characterized C/g-C_3N_4/PVDF composite membrane material.

The mapping images in Figures 2 d, e, g, and Figure 3a confirm the presence of C, F, and N elements in the C/g-C_3N_4/PVDF composite. The results showed that the elements on the surface membrane were mainly C, F, and N, with contents of 39.61%, 56.44%, and 3.95%, respectively, indicating that the membrane agglomeration was a C/g-C_3N_4 catalyst.

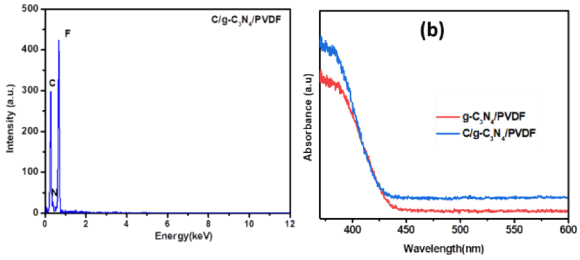

Figure 3. (a) EDX spectrum of C/g-C_3N_4/PVDF and (b) UV-Vis DRS spectra of g-C_3N_4/PVDF and C/g-C_3N_4/PVDF composite membrane.

The UV-Vis spectra of g-C_3N_4/PVDF and C/g-C_3N_4/PVDF composite membrane materials are shown in Figure 3b.

The results show that g-C_3N_4/PVDF and C/g-C_3N_4/PVDF composite membranes absorb in the ultraviolet region and extend into the visible. Compared with the g-C_3N_4/PVDF sample, the C/g-C_3N_4/PVDF composite membrane has a higher absorption intensity than the g-C_3N_4/PVDF in the visible region. This may be due to the presence of carbon in the composite.

As the photocatalytic activity of semiconductor materials is greatly affected by the recombination rate of photogenerated electron and hole pairs, the photoluminescence (PL) spectrum is used to evaluate this recombination ability. The photoluminescence spectra of PVDF, g-C_3N_4/PVDF, and C/g-C_3N_4/PVDF materials are presented in Figure 4.

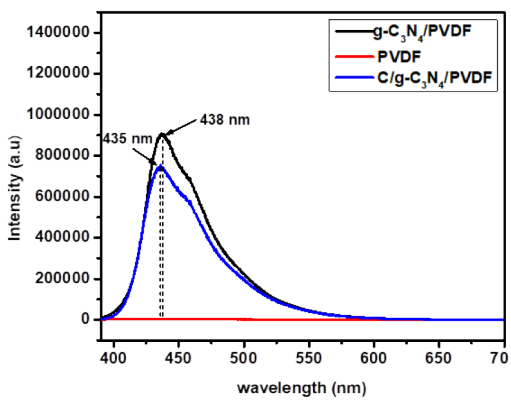

Figure 4. PL spectra of PVDF, g-C_3N_4/PVDF, and C/g-C_3N_4/PVDF materials.

PL spectra of PVDF, g-C_3N_4/PVDF, and C/g-C_3N_4/PVDF materials were conducted with an excitation wavelength of 390 nm. As shown in Figure 4, the C/g-C_3N_4/PVDF and C_3N_4/PVDF show peaks at 435 and 438 nm, respectively. However, the C/g-C_3N_4/PVDF composite membrane material exhibits lower emission intensity than g-C_3N_4/PVDF, which may be due to the addition of carbon helping improve the dispersion of the material. No significant PL intensity is observed across the entire measured PL spectrum for the PVDF membrane, indicating its limited adsorption properties. Consequently, the luminescence intensity is very low and nearly non-existent. Since PVDF does not have inherent luminescence, the observed PL shift is attributed to the excitation effect induced by adding g-C_3N_4 and carbon.[29] The PL spectral results suggest that the recombination rate of electron-hole pairs in C/g-C_3N_4/PVDF is lower than in g-C_3N_4/PVDF. This enhanced electron separation in C/g-C_3N_4/PVDF creates favorable conditions for photogenerated electrons to diffuse to the catalyst surface, where they interact with adsorbed H_2O or O_2 molecules to generate active free radicals, thus improving the efficiency of pollutant treatment.

3.2. Photocatalytic performance

The results of the photocatalytic evaluation for PVDF, g-C_3N_4/PVDF, and C/g-C_3N_4/PVDF are shown in Figure 5a.

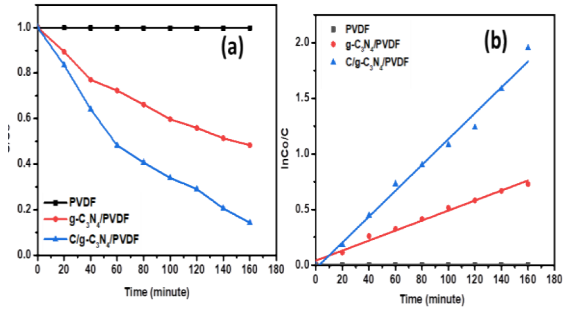

Figure 5. (a) RhB decomposition and (b) pseudo-first-order kinetic model under visible light of g-C_3N_4/PVDF, C/g-C_3N_4, and C/g-C_3N_4/PVDF materials.

After 160 minutes of illumination, the RhB decomposition efficiency of the C/g-C_3N_4/PVDF composite membrane reached 89%, which was higher than that of C_3N_4/PVDF, which achieved efficiencies of 45.92%. For the RhB solution of the PVDF fiber membrane without catalyst powder, the concentration remained

https://doi.org/10.52111/qnjs.2025.19310

almost unchanged under dark adsorption and light conditions, and the adsorption of RhB in the dark was only 2.09%, which also shows that pure PVDF has no degradation ability for RhB under natural conditions. After the PVDF membrane was laminated with g-C_3N_4 or C/g-C_3N_4 composite, the adsorption capacity of RhB in the dark was enhanced, which also shows that part of the g-C_3N_4 or C/g-C_3N_4 catalyst was exposed on the membrane, thereby increasing the dark adsorption of RhB by the composite membrane. Therefore, the ability to decompose RhB will increase when exposed to light. This is consistent with the results discussed in PL and UV-Vis DRS spectra.

These results highlight the potential of g-C_3N_4/PVDF, C/g-C_3N_4/PVDF composite for practical membrane-based environmental treatment applications.

Furthermore, Figure 5b presents the fitting results of the photoreduction kinetic curves of RhB over different samples using the first-order reaction kinetics equation of $-\ln(C/C_o)=kt$. The maximum photoreduction rate constant of RhB over the C/g-C_3N_4/PVDF photocatalysis membrane is 0.0116 min^{-1}, which is about 2.6 times that of g-C_3N_4/PVDF (0.0045 min^{-1}). These results demonstrate that the synergistic effect of C/g-C_3N_4 and PVDF membrane improves the photoreduction performance of g-C_3N_4.[30]

3.3. Photocatalytic cycle experiment

The photocatalytic stability of the C/g-C_3N_4/PVDF composite membrane was analyzed by conducting a cycle stability experiment (Figure 6).

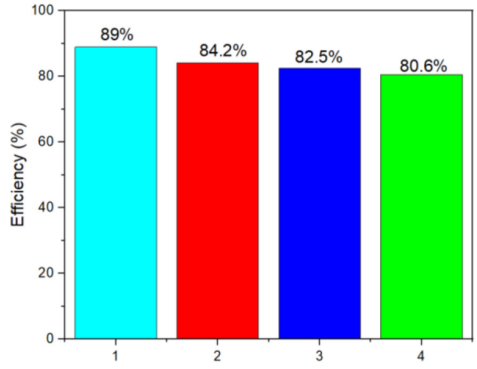

Figure 6. Reusability of C/g-C_3N_4/PVDF membrane materials.

The results showed that the removal rate of RhB was 89% when the C/g-C_3N_4/PVDF composite membrane was used for catalytic degradation once. After ultrasonic cleaning of the recovered composite membrane, the degradation efficiency of RhB was 84.2% (second time) after 160 min of illumination. After repeating twice, the removal rates of RhB were 82.5% (third time) and 80.6% (fourth time), respectively. This shows that the membrane can effectively photocatalytically degrade RhB and can be reused through water-washing regeneration. After regeneration three times, the membrane maintained a high efficiency, indicating that the prepared C/g-C_3N_4/PVDF membrane has efficient photocatalytic and excellent regeneration performance for RhB.

4. CONCLUSION

The phase inversion method successfully synthesized g-C_3N_4/PVDF, C/g-C_3N_4/PVDF materials. The C/g-C_3N_4/PVDF composite membrane exhibits excellent photocatalytic activity under visible light with an efficiency of 89% after 160 min of illumination, which was superior to those of g-C_3N_4/PVDF and pure PVDF membranes (45.92% and 2.09%, respectively). At the same time, it has stable recycling performance. Even after 4th recycling, the degradation efficiency reaches 80.6%, indicating that the C/g-C_3N_4/PVDF composite membrane has broad application prospects in the photocatalytic degradation of organic dyes in wastewater.

Acknowledgments

This research is funded by the Vietnamese Ministry of Education and Training under Grant B2023-DQN-02.

REFERENCES

1. K. N. Harish, H. S. B. Naik, P. N. P. Kumar, R. Viswanath. Optical and photocatalytic properties of solar light active Nd-substituted Ni ferrite catalysts: for environmental protection, *ACS*

Sustainable Chemistry & Engineering, **2013**, *1*(9), 1143-1153.

2. J. Chen, C. S. Poon. Photocatalytic cementitious materials: influence of the microstructure of cement paste on photocatalytic pollution degradation, *Environmental Science & Technology,* **2009**, *43*(23), 8948-8952.

3. J. Benner, D. E. Helbling, H. P. E. Kohler, J. Wittebol, E. Kaiser, C. Prasse, T. A. Ternes, C. N. Albers, J. Aamand, B. Horemans. Is biological treatment a viable alternative for micropollutant removal in drinking water treatment processes?, *Water Research,* **2013**, *47*(16), 5955-5976.

4. D. Kanakaraju, B. D. Glass, M. Oelgemöller. Advanced oxidation process-mediated removal of pharmaceuticals from water: a review, *Journal of Environmental Management,* **2018**, *219*, 189-207.

5. M. Antonopoulou, C. Kosma, T. Albanis, I. Konstantinou. An overview of homogeneous and heterogeneous photocatalysis applications for the removal of pharmaceutical compounds from real or synthetic hospital wastewaters under lab or pilot scale, *Science of the Total Environment,* **2021**, *765*, 144163.

6. J. Meijide, G. Lama, M. Pazos, M. Sanromán, P. S. Dunlop. Ultraviolet-based heterogeneous advanced oxidation processes as technologies to remove pharmaceuticals from wastewater: an overview, *Journal of Environmental Chemical Engineering,* **2022**, *10*(3), 107630.

7. J. Wen, J. Xie, X. Chen, X. Li. A review on g-C_3N_4-based photocatalysts, *Applied Surface Science,* **2017**, *391*, 72-123.

8. S. Zhou, Y. Liu, J. Li, Y. Wang, G. Jiang, Z. Zhao, D. Wang, A. Duan, J. Liu, Y. Wei. Facile in situ synthesis of graphitic carbon nitride (g-C_3N_4)-N-TiO_2 heterojunction as an efficient photocatalyst for the selective photoreduction of CO_2 to CO, *Applied Catalysis B: Environmental,* **2014**, *158*, 20-29.

9. X. Wang, Y. Yang, F. Li, Y. Xue, R. Liu, Y. Hao. In situ microwave-assisted synthesis of porous N-TiO_2/g-C_3N_4 heterojunctions with enhanced visible-light photocatalytic properties, *Industrial & Engineering Chemistry Research,* **2013**, *52*(48), 17140-17150.

10. C. Miranda, H. Mansilla, J. Yáñez, S. Obregón, G. Colón. Improved photocatalytic activity of g-C_3N_4/TiO_2 composites prepared by a simple impregnation method, *Journal of Photochemistry and Photobiology A: Chemistry,* **2013**, *253*, 16-21.

11. S. Cao, J. Low, J. Yu, M. Jaroniec. Polymeric photocatalysts based on graphitic carbon nitride, *Advanced Materials,* **2015**, *27*(13), 2150-2176.

12. Y. Deng, J. Liu, Y. Huang, M. Ma, K. Liu, X. Dou, Z. Wang, S. Qu, Z. Wang. Engineering the photocatalytic behaviors of g/C_3N_4-based metal-free materials for degradation of a representative antibiotic, *Advanced Functional Materials,* **2020**, *30*(31), 2002353.

13. F. Yang, G. Ding, J. Wang, Z. Liang, B. Gao, M. Dou, C. Xu, S. Li. Self-cleaning, antimicrobial, and antifouling membrane via integrating mesoporous graphitic carbon nitride into polyvinylidene fluoride, *Journal of Membrane Science,* **2020**, *606*, 118146.

14. T. T. Zhou, F. H. Zhao, Y. Q. Cui, L. X. Chen, J. S. Yan, X. X. Wang, Y. Z. Long. Flexible TiO_2/PVDF/g-C_3N_4 nanocomposite with excellent light photocatalytic performance, *Polymers,* **2019**, *12*(1), 55.

15. I. Kolesnyk, J. Kujawa, H. Bubela, V. Konovalova, A. Burban, A. Cyganiuk, W. Kujawski. Photocatalytic properties of PVDF membranes modified with g-C_3N_4 in the process of Rhodamines decomposition, *Separation and Purification Technology,* **2020**, *250*, 117231.

16. J. Huang, J. Hu, Y. Shi, G. Zeng, W. Cheng, H. Yu, Y. Gu, L. Shi, K. Yi. Evaluation of self-cleaning and photocatalytic properties of modified g-C_3N_4 based PVDF membranes driven by visible light, *Journal of Colloid and Interface Science,* **2019**, *541*, 356-366.

17. N. T. Lan, P. T. T. Trang, N. T. Lam, L. T. T. Lieu, N. L. Tuan, N. T. Hoang, V. Vien, D. Q. Khieu. Activated carbon/g-C_3N_4 /H_2O_2 system with enhanced photocatalytic activity for Rhodamine-B degradation under the visible

https://doi.org/10.52111/qnjs.2025.19310

light, *Environmental Engineering Research*, **2024**, *30*(1), 240121.

18. L. Valenzuela, M. Pedrosa, A. Bahamonde, R. Rosal, A. T. Pinto, C. G. Silva, J. L. Faria, A. M. Silva. Carbon nitride–PVDF photocatalytic membranes for visible-light degradation of venlafaxine as emerging water micropollutant, *Catalysis Today,* **2023**, *418*, 114042.

19. S. Vidhate, A. Shaito, J. Chung, N. A. D'Souza. Crystallization, mechanical, and rheological behavior of polyvinylidene fluoride/carbon nanofiber composites, *Journal of Applied Polymer Science,* **2009**, *112*(1), 254-260.

20. R. Song, D. Yang, L. He. Effect of surface modification of nanosilica on crystallization, thermal and mechanical properties of poly (vinylidene fluoride), *Journal of Materials Science,* **2007**, *42*, 8408-8417.

21. B. Zhu, P. Xia, Y. Li, W. Ho, J. Yu. Fabrication and photocatalytic activity enhanced mechanism of direct Z-scheme g-C_3N_4/Ag_2WO_4 photocatalyst, *Applied Surface Science,* **2017**, *391*, 175-183.

22. L. Zhu, Y. Wang, F. Hu, H. Song. Structural and friction characteristics of g-C_3N_4/PVDF composites, *Applied Surface Science,* **2015**, *345*, 349-354.

23. J. Liu, T. Zhang, Z. Wang, G. Dawson,W. Chen. Simple pyrolysis of urea into graphitic carbon nitride with recyclable adsorption and photocatalytic activity, *Journal of Materials Chemistry,* **2011**, *21*(38), 14398-14401.

24. S. Yan, Z. Li, Z. Zou. Photodegradation performance of g-C_3N_4 fabricated by directly heating melamine, *Langmuir,* **2009,** *25*(17), 10397-10401.

25. N. Abzan, M. Kharaziha, S. Labbaf. Development of three-dimensional piezoelectric polyvinylidene fluoride-graphene oxide scaffold by non-solvent induced phase separation method for nerve tissue engineering, *Materials & Design,* **2019**, *167*, 107636.

26. M. Kim, Y. S. Wu, E, C. Kan, J. Fan. Breathable and flexible piezoelectric ZnO@ PVDF fibrous nanogenerator for wearable applications, *Polymers,* **2018**, *10*(7), 745.

27. K. Tan, W. Gan, T. Velayutham, W. A. Majid. Pyroelectricity enhancement of PVDF nanocomposite thin films doped with ZnO nanoparticles, *Smart Materials and Structures,* **2014**, *23*(12), 125006.

28. Y. Cui, L. Yang, M. Meng, Q. Zhang, B. Li, Y. Wu, Y. Zhang, J. Lang, C. Li. Facile preparation of antifouling gC_3N_4/Ag_3PO_4 nanocomposite photocatalytic polyvinylidene fluoride membranes for effective removal of rhodamine B, *Korean Journal of Chemical Engineering,* **2019**, *36*, 236-247.

29. N. Nikooe, E. Saljoughi. Preparation and characterization of novel PVDF nanofiltration membranes with hydrophilic property for filtration of dye aqueous solution, *Applied Surface Science,* **2017**, *413*, 41-49.

30. Z. Vilamova, L. Svoboda, J. Bednar, Z. Simonova, R. Dvorsky, C. Silva, J. Faria. Enhancing photocatalytic g-C_3N_4/PVDF membranes through new insights into the preparation methods, *Polymer,* **2024**, 127238.

31. H. Wang, R. Gong, X. Qian. Preparation and characterization of TiO_2/g-C_3N_4/PVDF composite membrane with enhanced physical properties, *Membranes,* **2018**, *8*(1), 14.